JOURNAL OF PROPULSION AND POWER
Vol. 20, No. 1, January–February 2004

Ultrasonic Properties of Propellant Ingredients

Makoto Kohga*
National Defense Academy, Kanagawa 239-8686, Japan
and
Robert A. Frederick Jr.† and Marlow D. Moser‡
University of Alabama in Huntsville, Huntsville, Alabama 35899

Ultrasonic, pulse-echo transducers send acoustic waves through a solid propellant to determine the web thickness and the burning rate. The acoustic speed in the propellant increases with increasing pressure and must be quantified to make accurate burning-rate calculations. This experimental work determined the speed of sound as a function of pressure for cured and uncured binder materials hydroxyl-terminated polybutadiene (HTPB) and polytetrahydrofuran (PTHF) and epoxy. A nitrogen system pressurized the 3-cm-diam, 2–47-mm-thick, cylindrical samples to pressures of 15 MPa at pressurization rates of 2 or 14 MPa/s. The results show that the acoustic velocity of cured HTPB, PTHF, and epoxy are 1510, 1650, and 2600 m/s, respectively, at 6.9 MPa. Velocities for uncured HTPB and PTHF range from 1560 to 1610 m/s. The uncertainty is estimated at 1% for a 15-mm sample thickness. The pressure sensitivity is linear above 3 MPa at 1.4–4.3 m/s · MPa. A study of cured and uncured HTPB samples having lengths from 2 to 47 mm revealed a 20% variation in the sound speed at sample lengths below 10 mm. This effect could be the result of a measurement bias for the cured samples and surface tension for the uncured samples.

Nomenclature

a	=	pressure coefficient of sound speed, m/s · MPa
a_τ	=	pressure coefficient of echo time, μs/MPa
b	=	intercept of sound speed ($P = 0$), m/s
b_τ	=	intercept of echo time ($P = 0$), μs
C	=	speed of sound, m/s
C_R	=	reference speed of sound at 6.9 MPa, m/s
k_p	=	pressure correction coefficient, Pa^{-1}
k_t	=	temperature correction coefficient, K^{-1}
L_{bias}	=	bias in measurement of sample thickness, cm
L_s	=	sample thickness, cm
M	=	molecular weight, kg/kg · mole
m	=	coefficient in Eq. (2), μs/V
n	=	coefficient in Eq. (2), μs
P	=	pressure, MPa
T	=	temperature, K
V_{EDUM}	=	output voltage of the electric device for ultrasonic measurement (EDUM), V
Z_R	=	reference acoustic impedance at 6.9 MPa, kg/s · m^2
ρ	=	density of material, g/cm^3
τ	=	propagation time, μs
τ_{bias}	=	bias in sample echo time, μs
τ_3	=	propagation time of third echo, μs
τ_4	=	propagation time of fourth echo, μs

Introduction

THE ultrasonic pulse-echo method determines solid propellant thickness during combustion as a function of time.[1–7] An ultrasonic wave is transmitted through a coupling material to the base of the propellant sample. The wave propagates through the propellant and reflects off the burning surface. The reflected wave (echo) returns to the transducer by the same path. A simple mathematical relation determines the sample length using this propagation time of the echo and the assumed sound speeds in the coupling and sample material. The time derivative of the distance measurements provides the burning rate of the propellant.

In laboratory applications, the propellant sample is burned in a closed bomb.[8] The combustion gases pressurize the chamber to levels of 40 MPa. For example, a 30-g sample pressurizes a closed bomb at 20 MPa/s over a 20 MPa pressure range. The pressure level and pressurization rate are mainly dependent on the sample size, burning rate, and bomb volume.

Past researchers have documented the sound speed for several propellants and ingredients. Table 1 shows the nominal values of sound speed and the frequency of the ultrasonic transducer. The nominal sound speed and echo time are not used alone to determine the propellant thickness during combustion. ONERA researchers[9] proposed a pressure and temperature dependence of the sound speed in the propellant as

$$C_{\text{ref}}/C = \{1 - k_p(P - P_{\text{ref}})\}\{1 + k_t(T - T_{\text{ref}})\} \qquad (1)$$

where C_{ref} is the reference speed of sound at P_{ref} and T_{ref}. They reported values of the correction coefficient k_p as 3×10^{-9} Pa^{-1} and k_t is 2.9×10^{-3}/K for an ammonium perchlorate polybutadiene propellant.[9] This means that the sound speed varies by 3% for every 10-MPa change in pressure. The temperature effect is usually neglected, except in cases where the thermal profile beneath the burning surface is significant. Temperature effects have been considered in oxidizer[5] and hybrid fuel regression measurements.[6] In these cases, the burning rate is low, and the thermal layer is large and transient. Other researchers prefer to use echo time vs pressure calibrations to make the pressure correction without introducing the sound speed explicitly in the calculations.[10]

Because the pressure changes significantly during the closed-bomb combustion experiments, it is important to model the pressure effect accurately on the solid sound speed when calculating the propellant thickness. Omitting the pressure effect for a closed-bomb composite propellant test showed a 6% increase in the measured burning rate at 6.9 MPa. The magnitude of this bias correlates with the pressurization rates during the experiment. This paper examines the calibration process in detail using propellant binder materials. The specific results presented would apply to ultrasonic testing of

Received 13 August 2002; revision received 3 June 2003; accepted for publication 18 June 2003.

*Research Professor, Department of Applied Chemistry, 1-10-20 Hashirimizu, Yokosuka; kohga@mda.ac.jp. Member AIAA.

†Associate Professor, Department of Mechanical and Aerospace Engineering, UAH Propulsion Research Center; frederic@eb.uah.edu. Associate Fellow AIAA.

‡Assistant Research Professor, Department of Mechanical and Aerospace Engineering, UAH Propulsion Research Center; moser@mae.uah.edu. Member AIAA.

Table 1 Sound speeds in materials

Material	Frequency, MHz	C, at 20°C, m/s	Ref.
HNF[a]	5.00	3532	5
DX fuel	0.25	1960	13
Cured HTPB	0.25	1851	13
Cured HTPB	0.25	1687	14
AP[b]/HTPB/A	2.25	2075	15
L uncured AP/HTPB/AL	2.25	1915	15
PMMA[c]	2.50	2750	3, 16, 17, 18

[a]Hydrazinium nitroformate. [b]Aluminum powder. [c]Poly(methyl methacrylate).

Table 2 Binder formulations

Binder	$\bar{M}$, kg/kg · mole	Weight percentage, % Glycerin	IPDI	Binder
HTPB	3300		9.1	90.9
PTHF1	650	3.0	32.9	64.1
PTHF2	2900	0.9	10.2	88.9

fuels in hybrid rockets. The method presented and developed applies to solid propellants as well.

Approach

This experimental investigation evaluated the sound speed of binder/coupling materials as a function of pressure. The materials investigated included hydroxyl-terminated polybutadiene (HTPB), uncured and cured; polytetrahydrofuran (PTHF), uncured and cured; and epoxy, cured. The ultrasonic pulse-echo method measured the echo time of the binder samples and the coupling material as a function of pressure. Nitrogen gas loaded the samples at pressure levels up to 15 MPa. Variations in test conditions included the pressurization rate, the addition of an epoxy shell around the sample, and the sample length.

Sample Preparation

Table 2 shows the compositions of the HTPB and PTHF binder. The HTPB was mixed with isophorone diisocynate (IPDI) at about 60°C. The air and moisture in the mixture were removed by using a vacuum oven. The mixture was put into the oven at 90°C for approximately two days until it became hard. PTHF was mixed and cured with the same procedure. For PTHF, the glycerin/IPDI/PTHF mole ratios are 0.33/1.50/1.00. The epoxy, Araldite D, was cured at room temperature. Each cured sample was cast in 2.8-cm-diam disks that were nominally 1.5 cm thick. PTHF was softer than epoxy and harder than HTPB.

Test Apparatus

The data for the sound speed measurements are obtained at a combustion test facility. The facility consists of a combustion bomb, ultrasonic and pressure instrumentation, and a nitrogen pressurization system. Figure 1 shows a cross section of the combustion bomb. The combustion bomb consists of a pressure vessel and a removable sample holder. The sample holder contains a stainless-steel cylinder filled with a tapered epoxy coupling plug. The coupling material connects the ultrasonic transducer with the sample. The samples are bonded to the coupling material by applying a small layer of epoxy on the bottom of the sample, placing the assembly under vacuum to remove the gases, and allowing the assembly to cure at room temperature. Then, for some of the tests, the circumference of the sample was surrounded with an epoxy shell. This replicates the structural boundary conditions found in combustion tests where the epoxy shell prevents side burning. For the liquid samples, an epoxy tube was attached to the coupling plug. The uncured binder was metered into the cylinder using a syringe. The length was then deduced by dividing the volume by the tube area.

Figure 2 shows the ultrasonic instrumentation used for the testing. The tests were conducted with a 2.5-cm-diam Panametrics 1-MHzV102 1.0/1.0 ultrasonic transducer. The ultrasonic

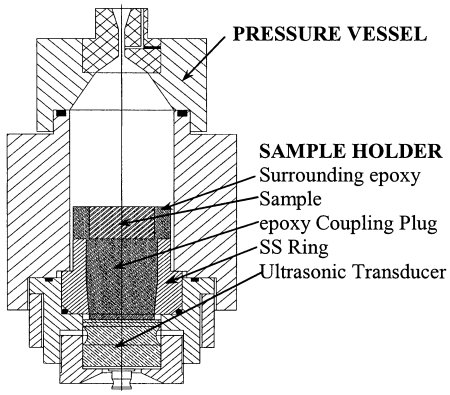

Fig. 1 Cross section of combustion chamber with sample holder.

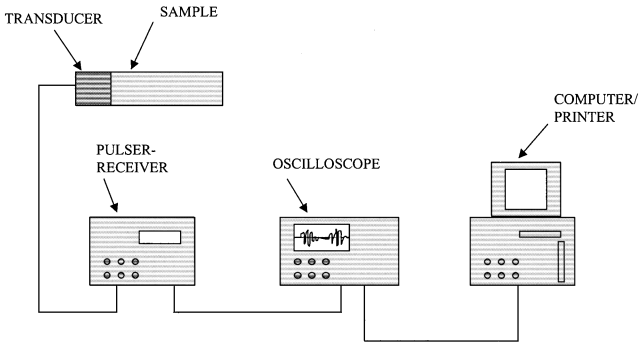

Fig. 2 Ultrasonic instrumentation.

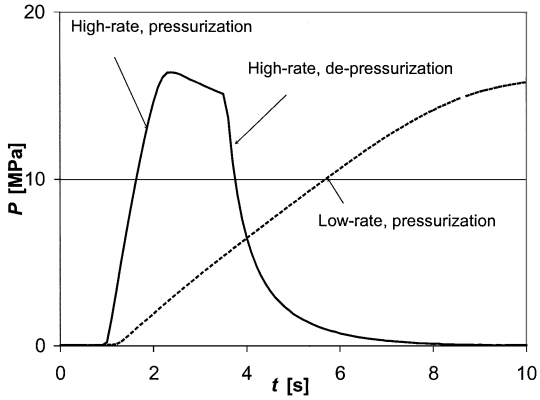

Fig. 3 Pressure vs time curves.

propagation times were measured using the electric device for ultrasonic measurement (EDUM).[11] The ultrasonic waves were observed with an HP54602B oscilloscope. The chamber pressure measurements were taken with a Setra Model 280E pressure transducer. A National Instruments analogue-to-digital (A/D) board with LabVIEW version 5.1 data acquisition software collected the transducer data. The data were taken at 1000 samples/s, and the input range of the 12-bit A/D board was set at −5–5 V.

A nitrogen system pressurized the bomb. Each sample was pressurized with nitrogen to 12–15 MPa. Because actual closed-bomb combustion test exhibited increasing pressures, the nitrogen was injected at two different rates to see the effect of pressurization rate. Figure 3 shows the relationship between pressure P and time t. The high rate was approximately ±13.8 MPa/s (pressurization and depressurization), and the low rate was approximately +2.4 MPa/s (pressurization only). The testing temperature was 23°C.

For the sound speed results, only the pressurization data were analyzed for the solid samples because closed-bomb experiments pressurize the bomb. The acoustic echo time data during depressurization are presented. The acoustic data for the liquid samples were measured at atmospheric pressure, 3.5, 6.9, and 13.8 MPa. The data

under high- and low-pressurization rates were not measured because the liquid splashed in the cylinder during depressurization.

Analysis, Results, and Discussion

Coupling Material

The ultrasonic echoes of the coupling material were first measured without a sample. Four different epoxy-plug/steel-cylinder assemblies were used in this study. Because each assembly had slightly different dimensions and composition, they were characterized individually.

Figure 4 shows the ultrasonic echoes at 3.4 and 10.3 MPa for one of the holders. The first wave is the signal from the transducer. The second wave is the echo from the bottom of the transducer. It travels through the transducer backing material and is reflected back to the ultrasonic element, where it is detected. The third wave represents the echo from the coupling material surface. A portion of this third wave reflects at the transducer/sample interface back toward the coupling material surface. The fourth echo represents the return of this reflected wave. The 3.4 and the 10.3 MPa data are superimposed in Fig. 4 because the curve moves less than the width of the line.

The EDUM produces a voltage proportional to the echo time of a selected echo. An electronic mask brackets a time window to track the selected wave. The echo time is determined as the first zero crossing of the selected wave, in this case, echo 3, after it achieves a threshold voltage. A linear relationship exists between the EDUM output voltage and the propagation time

$$\tau = mV_{\text{EDUM}} + n \tag{2}$$

The m and n are obtained by pretest calibrations. The propagation time τ is the total propagation time it takes for the pulse to pass through the coupling material to the surface and return. It is the period between the start of the input signal, $t = 0$ and the third-echo, zero crossing. Figure 5 shows the resulting propagation time of the coupling material as a function of pressure. The τ_3 decreased gradually as the pressure increased. The data above 2 MPa are

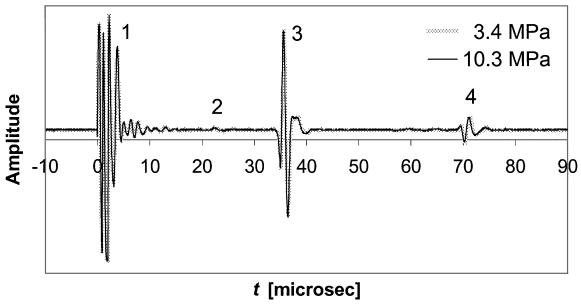

Fig. 4 Ultrasonic echoes of coupling material.

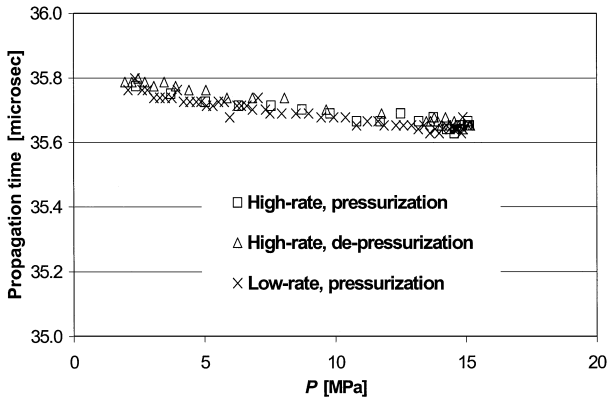

Fig. 5 Propagation time and pressure as a function of pressurization rate for coupling material.

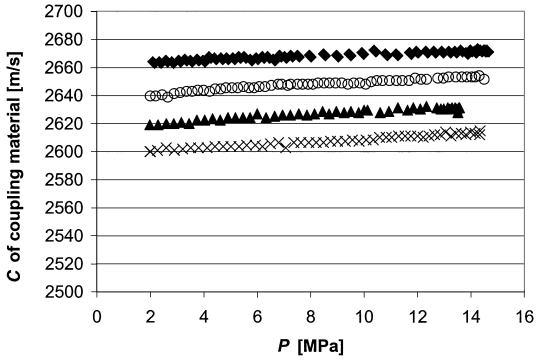

Fig. 6 Ultrasonic velocity of coupling material.

regression fit with

$$\tau_3 = a_\tau P + b_\tau \tag{3}$$

The resulting curve fit for the data shown gives $a_\tau = -0.009\ \mu$s/MPa and $b_\tau = 35.8\ \mu$s.

Figure 6 shows the calculated ultrasonic velocity of the coupling material as a function of pressure for each of the sample holder assemblies. The ultrasonic velocity C was estimated using the sample length and the surface echo time,

$$C = 2L_s/\tau_3 \tag{4}$$

The length of the coupling material L_s was measured with a dial gauge accurate to 0.025 mm. The thickness measurement was taken at over a time interval to see if the material compressed with time and the amount it compressed. The apparent C increased gradually as P increased, and this relationship followed a straight line above 2 MPa. The data above 2 MPa are curve fit with

$$C = aP + b \tag{5}$$

The a and b of the coupling material range from 0.654 to 0.911 m/s · MPa and from 2523 to 2691 m/s, respectively. The pressure coefficient is relatively small for the epoxy. The variations of these coefficients in Eq. (5) among the four different sample holders results from the batch-to batch variations in the epoxy properties and variations in the geometry among stainless-steel rings. The rings had slight variations in geometry. The epoxy in the holders were cast from different mixes.

These data were also used to calculate reference values of acoustic speed C_R and impedance Z_R. The reference condition is the value at 6.9 MPa. The C_R is the range of 2606–2668 m/s. The reference acoustic impedance is

$$Z_R = \rho C_R \tag{6}$$

The ρ of the coupling material was 1.14 g/cm^3. The Z_R of the coupling material varies from 2.97 to 3.04×10^6 kg/s · m^2.

The acoustic impedance has direct influence on the wave transmission between two materials. Mismatches in the acoustic impedance promote reflection. A discontinuity in Z_R is good at the sample surface to promote the surface echo. However, at the coupling/ sample interface, the acoustic impedances of the two materials should be similar to promote the transmission of the wave through the interface.

Solid Samples Without Surrounding Epoxy

The cured HTPB, PTHF, and epoxy samples were first tested without the surrounding epoxy. This provided a free structural boundary around the circumference of the samples. The next set of tests examined the samples with a shell of surrounding epoxy. The motivation was to compare these results for the different structural boundary conditions.

Figure 7 shows the ultrasonic echoes at 3.4 and 10.3 MPa for the different cured sample materials. The first wave is the signal from

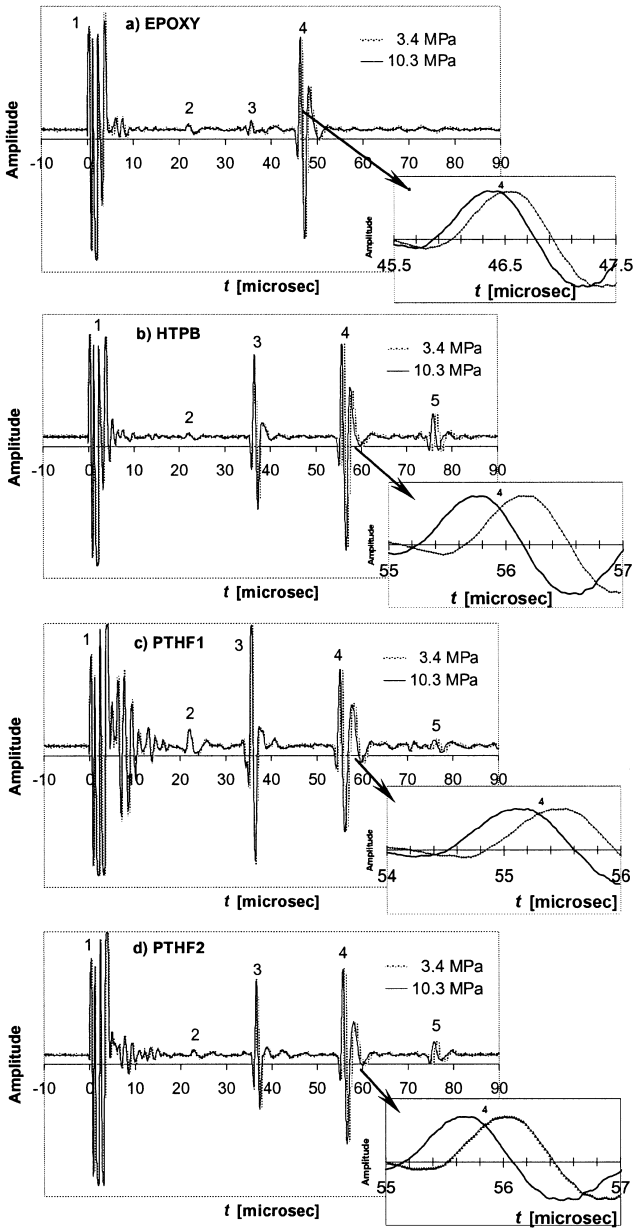

Fig. 7 Ultrasonic echoes without surrounding epoxy.

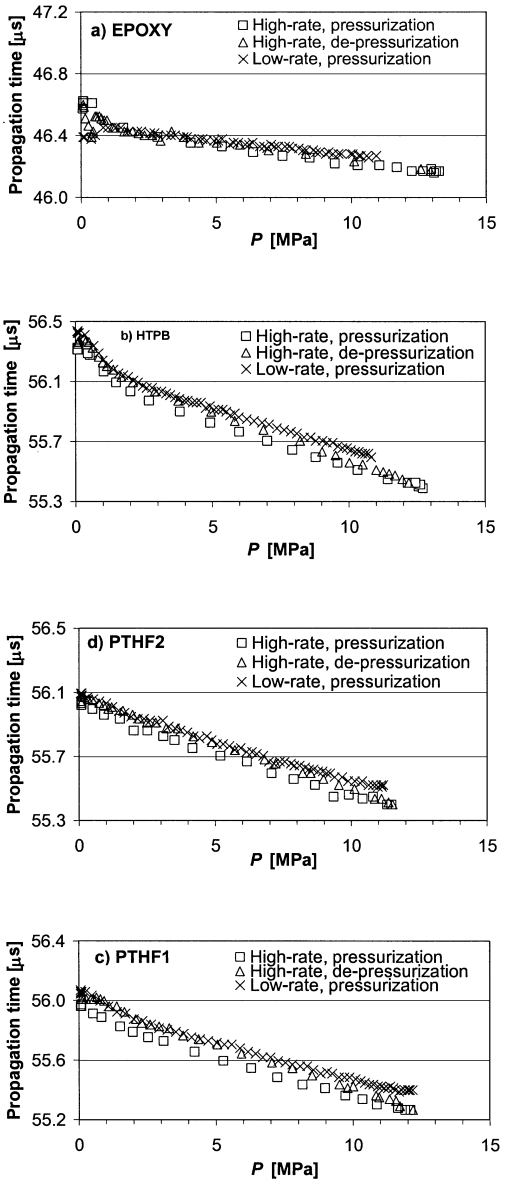

Fig. 8 Propagation time and pressure as a function of pressurization rate for each solid material.

the transducer. The second wave is the echo from the back of the transducer. The third wave is the echo from the coupling/sample interface. The fourth wave is the echo from the sample surface. This is a result of the poor impedance match at the coupling material/sample interface for these samples.

The 10.3 MP and 3.4 MPa curves appear superimposed in Figs. 7a–7d. An enlargement of the fourth wave is overlaid in of Figs. 7a–7d to magnify the increased echo time at the higher pressure level. These insets show that the binder echoes shift more than the epoxy echo for the same pressure difference.

The third wave in Fig. 7 represents the binder/coupling interface echo. This wave was very small for the epoxy (Fig. 7a) compared with HTPB, PTHF1, and PTHF2, (Figs. 7b–7d). Because the acoustic impedance of the coupling plug and the sample are the same for epoxy, only a slight echo comes from the bond discontinuity between them. For the binders, the interface echo is much larger. This results from the impedance mismatch between the coupling and the sample and the quality of the bond between them. For example, the PTHF1 interface echo is larger that that of the PTHF2 sample. Because the Z of the samples are similar, the difference must be in the bond quality. Also notice that the amplitude of the surface echo is lower for the PTHF1 sample than for the PTHF2 sample. More energy is lost at the interface in the PTHF1 sample. Good bonding, therefore, increases the signal strength.

Figure 8 shows the resulting propagation time vs P for each cured material. The pressure and the pressurization rate effects were small for the epoxy compared to the other samples. The HTPB, PTHF1, and PTHF2 responded differently to the high-rate pressurization and depressurization. The echo time increased slightly during depressurization for the high-rate tests. The low-rate pressurization echo times agreed more closely with the high-rate depressurization echo times. The relationship between the echo time and P became nonlinear below 2–3 MPa. The shifts on the high-rate tests could be the influence of sample heating.

The acoustic speed in the sample itself as a function of pressure is determined by subtracting the sample echo times and the coupling material echo times. The propagation time to pass through sample is the period between the third echo and the fourth echo. The C of the sample was obtained by

$$C = 2L_s/2 = 2L_s/(\tau_4 - \tau_3) \tag{7}$$

Only the high- and low-rate pressurization data above 3 MPa were used in the calculation of the acoustic velocity. The τ_3 was determined using the regression constants from Eq. (3). The τ_4 was determined from the data points in Fig. 8.

Table 3 Coefficient in ultrasonic velocity of binder materials

Binder material	Without surrounding epoxy			With surrounding epoxy		
	a, m/s · MPa	b, m/s	r^2	a, m/s · MPa	b, m/s	r^2
EPOXY	2.204	2604	0.89	1.467	2575	0.71
HTPB	3.552	1483	0.99	3.774	1490	0.99
Liquid HTPB	——	——	——	3.488	1626	——
PTHF1	3.348	1631	0.99	3.610	1613	0.99
Liquid PTHF1	——	——	——	3.640	1593	——
PTHF2	3.144	1670	0.99	3.724	1662	0.98

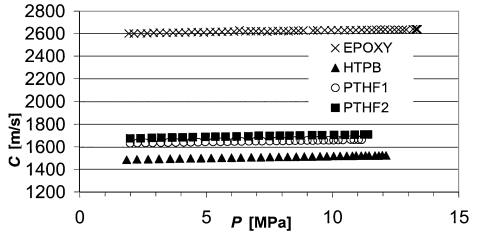

Fig. 9 Ultrasonic velocity of binder material without surrounding epoxy.

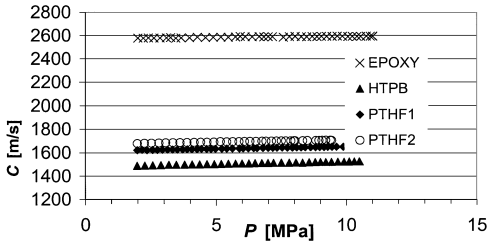

Fig. 10 Ultrasonic velocity of binder material with surrounding epoxy.

Figure 9 shows the ultrasonic velocity of binder materials without surrounding epoxy. The C increased gradually as P increased. This relationship followed a straight line in the pressure range selected.

Binder Material with Surrounding Epoxy

A 10-mm-thick epoxy ring was cast around the samples for these experiments. This duplicates the initial condition of propellant tests with combustion. For the combustion experiments, the epoxy serves as an inhibitor. More important for these experiments, it represents a structural boundary condition that might influence the results.

For all of the samples, the ultrasonic echoes and the output voltage V_{EDUM} vs P data were almost the same as those of the binder materials without the surrounding epoxy. The data reduction was conducted in the same manner as described earlier. Figure 10 shows the ultrasonic velocity of the samples with the surrounding epoxy.

Summary of Sound Speed Results

Table 3 shows the sound speed coefficients that correspond to Eq. (5). Table 3 also shows the coefficient of determination, r^2, for each data fit. The uncured materials could not be tested without the surrounding tube.

The b represent the ultrasonic velocity extrapolated to atmospheric pressure. Comparing the results for each material with and without epoxy showed no real difference. The maximum differences of b for each sample of similar material is 1%. Compared among the materials, the b of epoxy was the highest and that of HTPB was the lowest. The b of PTHF were almost constant.

The a represent the pressure sensitivity of the ultrasonic velocity. It is easier for a soft material to compress under pressure. Therefore, a will be larger for a softer material. The a of HTPB, PTHF1, and PHF2 binders varied by $\pm 10\%$ for all of the tests. The a of the epoxy dropped 50% when additional surrounding epoxy was added. The pressure sensitivity of the ultrasonic velocity for HTPB, PTHF1, and PHF2 binders was larger than that for epoxy.

Table 4 Properties of materials tested

Sample	ρ, g/cm^3	C_{R1},[a] m/s	C_{R2},[b] m/s	Z_{R1},[a] kg/s · m^2	Z_{R2},[b] kg/s · m^2
EPOXY	1.14	2619	2585	2.99×10^6	2.95×10^6
HTPB	0.93	1508	1516	1.40×10^6	1.41×10^6
Liquid HTPB	0.90	——	1640	——	1.48×10^6
PTHF1	1.04	1654	1638	1.72×10^6	1.70×10^6
Liquid PTHF1	0.98	——	1618	——	1.59×10^6
PTHF2	0.96	1692	1688	1.62×10^6	1.62×10^6

[a]Reference pressure = 6.9 MPa and no surrounding epoxy.
[b]Reference pressure = 6.9 MPa with surrounding epoxy.

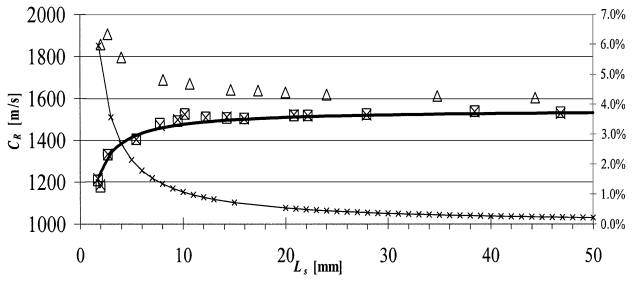

Fig. 11 Reference sound speed for HTPB as a function of length: ——, calculated with time bias of 0.6 ms; □, with surrounding epoxy; —×—, uncertainty in C; ×, without surrounding epoxy; and △, liquid HTPB.

Table 4 shows the reference acoustic speed and acoustic impedance of each material. The density of each material is shown. The uncertainty in the sound speed[12] was determined at about 1%, and the range of the uncertainty of the acoustic impedance was 2–3%.

Effect of Sample Length: HTPB

The effect of sample length on the acoustic properties was investigated for cured and uncured HTPB. The motivation for these experiments was to determine if there might be a length effect associated with the pressure sensitivity. Several samples were cast to produce lengths that varied from 1.7 to 47 mm. Measurements were taken with and without surrounding epoxy. Liquid samples were prepared and examined over the same range.

Figure 11 shows the reference sound speed C_R as a function of sample length for these tests. The measured speed of sound varied by 20% over the range of lengths tested. The surrounding epoxy did not have a significant effect. The reference sound speed of the uncured material increased by about 20% as the length decreased. The cured material sound speed decreased by about 20% as the length decreased.

Several hypotheses for possible causes of the acoustic velocity change with length were considered for the cured samples. The first one speculates that the measurement is accurate. The others quantify possible measurement biases. The following equation is modified to introduce a length-measurement bias and a time-measurement bias,

$$C = 2\frac{(L_s + L_{\mathrm{bias}})}{(\tau_{\mathrm{bias}} + \tau_4 - \tau_3)} \tag{8}$$

as a framework for the discussion.

The first possible explanation is that there are no biases and that the sound speed does change by over 20% as the length decreases. Batch-to-batch variation in properties is a possible cause. However, several samples were cast from the same batch of propellants. Moreover, the batch-to-batch variation should not correlate with the sample length. Another possibility is that the sound speed near one surface of the sample is lower than the bulk material. This could be a casting effect. It could also be a thermal effect. As the bomb pressurizes, the gas temperature rises, and heat is transferred to the sample surface. The end of the sample heats, which results in a lower acoustic speed in the heated region. Assuming this end effect to be a constant depth, its influence would be magnified at shorter sample lengths.

The second hypothesis is that the uncertainty of the measurement increases with decreasing thickness. The calculated measurement uncertainty[12] does increase with decreasing thickness. For the shortest length, the uncertainty in sound speed goes to 6%, as shown in Fig. 11. However, as before, the random uncertainty would be as likely to cause values above the nominal value as below it. The data show a consistent bias below the nominal value. In addition, the percentage deviation in the sound speed is larger that the estimated uncertainty.

The third hypothesis is a constant sound speed and a bias in the measured length. Equation (8) shows that if the length bias is negative, that is, the sample is longer than measured, then the calculated sound speed will decrease with the decreasing sample length. Manipulating the data with different length bias assumptions yields a length bias of 0.38 mm to explain this trend. This explanation is possible because the length of the samples is measured with a spring-loaded touch gauge. Each thickness measurement was taken at timed intervals to see if the material compressed and, if so, the amount it compressed. The thickness of HTPB was measured first when the gauge was touched on the surface of the sample, L_1, and 1 h later, L_2. The $(L_1 - L_2)/L_2$ of the HTPB sample used in this experiment was less than 0.03. The L_s was determined by the average of the thickness, L_1 and L_2.

The fourth possible cause is a measurement bias in the echo time measurement. If the time measurement included a constant bias from the electronics or the detection point through the echo, it would not influence the results. Examining Eq. (8) reveals that the echo time for the sample is the difference between τ_4 and τ_3. An electronic bias, if consistent in the two measurements, would be subtracted out of the result.

A length-dependent time bias for the surface echo wave τ_4, however, could produce this result. This argument is plausible because the time separation of the surface echo and the interface echo decreases with thickness. If an interaction occurs between the two echoes that effectively "stretches" the zero crossing of the surface echo as it approaches the interface echo, a time bias will result. This time bias could also be introduced by length-dependent filtering of the acoustic wave. Because the propellant is a visco–elastic material, it acts as a low-pass filter. This means that the sample length will change the frequency composition of the waves that return to the surface and combine to form this echo. If this filtering stretches the wave, the time bias could be induced as a function of sample length.

To check the time-bias notion, the time bias was adjusted to match the results of the shortest sample. The time bias was assumed zero for the longest sample and 0.6 μs at the shortest length with a linear variation in between. The resulting sound speed plotted with this bias profile is plotted as a curve in Fig. 12 and correlates well with the data trend.

The sound speed data points of liquid HTPB are shown in Fig. 12. The measured speed of sound increases at lengths below 20 mm and is almost constant above that value. The sample length was converted into the volume as mentioned earlier. The surface of liquid is slightly curved down because of surface tension. The actual length was smaller than that calculated from the volume. The sound speeds in materials cited in Refs. 3, 5, and 13–18 are given in Table 1.

Conclusions

The acoustic characteristics of epoxy, HTPB, and PTHF were investigated to evaluate the sound speed as a function of pressure and length. The results for 1.5-cm cured samples show that the acoustic velocity of HTPB, PTHF, and epoxy are 1510, 1650, and 2600 m/s, respectively, at 6.9 MPa. The speed of sound for HTPB is comparable to the values cited in the literature in Table 1. The uncertainty of the sound speed is estimated at 1% for 1.5-cm samples. The measured speed of sound C of all of the samples increased linearly with pressure at pressure levels from 3 to 15 MPa. The acoustic speed is a weak function of pressure 1.4–4.3 m/s · MPa. The uncured HTPB had acoustic properties similar to the cured HTPB.

The results for the cured samples were not significantly changed by the addition of epoxy around the circumference of the sample or by the pressurization rates evaluated. The apparent acoustic speed and pressure relationship showed a sample-dependent, nonlinear behavior at pressure levels below 2 MPa.

The acoustic impedance Z_R of epoxy, HTTB, PTHF1, and PTHF2 are 2.97×10^6, 1.10×10^6, 1.71×10^6, and 1.62×10^6 kg/s · m^2, respectively. The sound speed gradually changed by 20% as the sample length decreased from 10 to 2 mm. A 20% decrease for the cured sample is likely due to a length or time bias in the measured data. The possible length bias is estimated at 0.38 mm, and the possible time bias is estimated at 0.6 μs. The 20% increase in reference sound speed at the short lengths for the uncured material can be explained by surface tension effects. Because of possible implication on burning-rate calculations, further evaluation is warranted to draw a conclusion from this unexpected trend of the cured material.

References

[1]Traineau, J., and Kuentzmann, P., "Some Measurements of Solid Propellant Burning Rates in Nozzleless Motors," *Journal of Propulsion and Power*, Vol. 2, No. 3, 1986, pp. 215–222.

[2]Murphy, J. J., and Krier, H., "Evaluation of the Ultrasound Technique for Solid-Propellant Burning-Rate Response Measurements," *Journal of Propulsion and Power*, Vol. 18, No. 2, 2002, pp. 641–651.

[3]Korting, P. A. O. G., den Hertog, E. H., and Schoyer, H. F. R., "Determination of the Regression Rate of Solid Fuels in Solid Fuel Combustion Chambers by Means of the Ultrasonic Pulse-Echo Technique. Part I. The Measurement Technique," Delft Univ. of Technology, Rept. LR-473, Delft, The Netherlands, April 1985.

[4]Dijkstra, F., Korting, P., and van der Berg, R., "Ultrasonic Regression Rate Measurement in Solid Fuel Ramjets," AIAA Paper 90-1963, July 1990.

[5]Louwers, J., Gadiot, G., Versluis, M., Landman, A. J., van der Meer, T., and Roekaerts, D., "Measurement of Steady and Non-Steady Regression Rates of Hydrazinium Nitroformate with Ultrasound," *Proceedings of the International Workshop on Measurement of Thermophysical and Ballistic Properties of Energetic Materials*, Politecnico di Milano, Milano, Italy, June 1998, pp. 22–24.

[6]Korting, P. A. O. G., and Schöyer, H. F. R., "Determination of the Regression Rate in Solid Fuel Ramjets by Means of the Ultrasonic Pulse Echo Method," *Proceedings of Heat Transfer in Fire and Combustion Systems*, edited by C. K. Law, Y. Jaluria, W. W. Yuen, and K. Miyasaka, HTD, Vol. 45, American Society of Mechanical Engineers, New York, Aug. 1985, pp. 347–353.

[7]Elands, P. J. M., Korting, P. A. O. G., Dijkstra, F., and Wijchers, T., "Combustion of Polyethylene in a Solid Fuel Ramjet: A Comparison of Computational and Experimental Results," AIAA Paper 88-3043, July 1988.

[8]Di Salvo, R., Dauch, F., Frederick, R. A., Jr., and Moser, M. D., "Direct Ultrasonic Measurement of Solid Propellant Ballistics," *Review of Scientific Instruments*, Vol. 70, No. 11, 1999, pp. 4418–4421.

[9]Traineau, J. C., and Kuentzmann, P., "Ultrasonic Measurements of Solid Propellant Burning Rates in Nozzleless Rocket Motors," *Journal of Propulsion and Power*, Vol. 2, No. 3, 1986, pp. 215–222; also AIAA Paper 84-1469, 1984.

[10]Dauch, F., Moser, M. D., Frederick, R. A., Jr., and Coleman, H. W., "Uncertainty Assessment of the Pulse-Echo Ultrasonic Burning Rate Measurement Technique," AIAA Paper 99-2224, June 1999.

[11]Cauty, F., "User's Manual of Electronic Device for Ultrasonic Measurements (EDUM) of Regression Rates of Solid Materials," Users Manual, ONERA Rept., Palaiseau, France, May 1995.

[12]Kohga, M., Frederick, R. A., Jr., and Moser, M. D., "Ultrasonic Properties of Propellant Ingredients," AIAA Paper 2002-3572, July 2002.

[13]Boardman, T. A., Porter, L. G., Brasfield, F. W., and Abel, T. M., "An Ultrasonic Fuel Regression Rate Measurement Technique for Mixture Ratio Control of a Hybrid Motor," AIAA Paper 95-3081, July 1995.

[14]Leahy, J. C., and Jackson, J. W., Jr., "Improvements in the Measurement of Hybrid Rocket Fuel Regression Rate using Ultrasonic Transducers," AIAA Paper 97-3082, July 1997.

[15]Cauty, F., and Démarais, J. C., "Ultrasonic Measurement of the Uncured Solid Propellant Burning Rate" ("Mesure par ultrasons de la vitesse de combustion d'um propergol non reticule"), *21st International Congress of ICT*, ONERA Rept. TP 1990-90, 1990, p. 15.

[16]Merkx, A. W., and van den Berg, R. P., "Instantaneous Solid Fuel Regression Rate Measurements at More than One Location—An Ultrasonic Pulse Echo Multiplexer System," Rept. LR-501, Rept. PML 1986-C76, SFCC Publ. No. 36, Prins Maurits Lab., Delft/Rijswijk, The Netherlands, Aug. 1986.

[17]Kono, R., "The Dynamic Bulk Viscosity of Polystyrene and Polymethyl Methacrylate," *Journal of the Physical Society of Japan*, Vol. 15, No. 4, 1960.

[18]North, A. M., Pethrick, R. A., and Phillips, D. W., "Ultrasonic Studies of Solid Poly (akyl methacrylates)," Polymer, Vol. 18, April 1977.